

PACS numbers: 42.55.Px; 42.60.Lh
DOI: 10.1070/QE2005v035n04ABEH002909

Simulation of the material gain in quantum-well InGaAs layers used in 1.06-μm heterolasers

D.V. Batrak, S.A. Bogatova, A.V. Borodaenko, A.E. Drakin, A.P. Bogatov

***Abstract*. The spectral profile of the optical gain and the spectral dependence of the coefficient characterising the variation in the refractive index with a carrier concentration are calculated using the three-band model for an active quantum-well InGaAs layer. A comparison of the theoretical results with the experimental data gave values of parameters allowing the numerical simulation of the material parameters of the active layer with a high degree of accuracy.**

Keywords: *semiconductor lasers, quantum well, heterolaser*.

1. Introduction

The state-of-the-art of manufacturing technology of heterostructures based on InGaAs/AlGaAs/GaAs compounds for semiconductor lasers emitting in the range 0.96 – 1.14 μm allows the fabrication of lasers with well-reproducible parameters, which suggests that uncontrollable technical imperfections only weakly affect their parameters. In this case, it can be hoped that the main parameters of the lasers, e.g., the threshold current and its temperature dependence, lasing efficiency and radiation wavelength, are determined entirely by the laser design and the material composition of the heterostructure layers on which they are based.

This opens new possibilities for simulating the radiation parameters of such lasers at the stage of their development. It is well known that such a simulation for semiconductor lasers is divided into two nearly independent problems. One of them is of electrodynamic type and is connected mainly with the solution of Maxwell's equations for a specific design of the laser cavity. As the initial parameter of this problem, the complex permittivity ε of layers at optical frequencies is used, which characterises the refractive indices of these layers and optical absorption or optical gain. In turn, the determination of ε, which is a material parameter of the medium, is the second problem in the simulation of laser characteristics. The determination of the real part of the permittivity or the refractive index of $In_xGa_{1-x}As$ and $Al_xGa_{1-x}As$ layers as a function of the composition x and the emission frequency is not a complicated problem since a large body of data has been accumulated by now (see, for example, [1, 2]) and quite convenient analytic approximations for this quantity have been obtained in [3, 4].

These data allow us to determine the refractive index in the required spectral range for given layer compositions in the structure with an accuracy up to the required digital place, which provides a nearly complete solution of the problem. As for the imaginary part of ε or the value of the gain (absorption) in the investigated structure, which we will call the material gain, the situation is not so good. As a rule, this quantity is almost constant for passive layers of the heterostructure and is determined by either scattering losses or interband absorption and absorption by free carriers. However, for active layers, the imaginary part of ε is a rapidly varying function of the frequency and carrier concentration.

Although a large number of theoretical and experimental works have been devoted to the determination of the material gain and the results of these investigations have been published in books and reviews (see, for example, [5, 6] and references therein), it cannot be stated that this problem has been solved completely. First, all theoretical works contain, as a rule, a large number of fitting parameters, e.g., the matrix element for dipole transitions, the form-factor for a homogeneously broadened line, effective masses for the stressed layers of multicomponent compounds, energy jumps at band edges, etc. On the one hand, this facilitates the fitting of experimental results; but on the other hand, it leads to considerable difficulties in simulation where it is desirable to reduce to a minimum the number of parameters whose values are not specified precisely.

Second, the physical situation itself characterising an active layer may be described inappropriately by the models used for calculations. This concerns the spatial profile of the band gap edges which may be deformed upon a change in the carrier concentration due to the spatial charge distribution. The conditions for a complete electron wave function at the heteroboundaries remain unclear, etc. All this does not rule out a situation when attempts at carrying out complex calculations involving mechanisms like band mixing, renormalisation of the forbidden band gap due to Coulomb interaction between free carriers or the dependence of the matrix element on the transition energy, etc., may appear as an unjustified excess over the accuracy of the model and thus raise doubts about its adequacy.

Further complications may be caused by the inconsistency in the literature in the formulas used for the

D.V. Batrak, A.E. Drakin, A.P. Bogatov P.N. Lebedev Physics Institute, Russian Academy of Sciences, Leninskii prosp. 53, 119991 Moscow, Russia; e-mail: bogatov@sci.lebedev.ru;
S.A. Bogatova, A.V. Borodaenko Moscow Institute of Physics and Technology (State University), Institutskii per. 9, 141700 Dolgoprudnyi, Moscow region, Russia

Received 22 October 2004
Kvantovaya Elektronika **35** (4) 316 – 322 (2005)
Translated by Ram Wadhwa

material gain (see, for example, Ref. [7] in this connection). From the practical point of view, this raises the issue of an alternative approach based on the simplest model with the smallest number of variable parameters which, nevertheless, approximates the experimental values of the material gain of the investigated structure with the desired degree of accuracy. Such an approach was used, for example, in [8, 9]. In particular, a semiempirical relation was obtained in [8] for the material gain in a quantum-well layer of GaInAsP at a wavelength of 1.55 μm for various carrier concentrations in the layer composition. Simple analytic relations were obtained on the basis of the two-band model in [9] for the material gain and correction to the refractive index as a function of the carrier concentration and the emission frequency. Although the results obtained in [9] can be attributed to any quantum-well $A^{III}B^{V}$ layer, they are applicable only at low temperatures under the condition that $k_B T$ is much smaller than the energy difference between the Fermi quasilayer and the band gap edge.

In this work, we use an alternative approach for the quantum-well InGaAs layer used as an active medium at temperatures close to 300 K. A simplified three-band model of the active medium was used to calculate the material gain.

2. Calculation of the gain in quantum-well active layer (quantum well)

Below we shall present the main relations for calculating the gain and refractive index spectra of a semiconductor quantum well within the framework of the simple, well-known three-band model, as well as their comparison with the experimental results. The band structure used for calculations is shown schematically in Fig. 1. Only one subband is considered for each energy band (conduction band, light hole band and heavy hole band) of the bulk semiconductor material, and the dispersion relation for each band is assumed to be parabolic and isotropic in the plane of the quantum well. Because of the so-called mass inversion effect, heavy holes (hh) have a lower effective mass than light holes (lh) in the plane of the quantum well. Therefore, the curves of the energy dependence on the wave vector (quasi-momentum) for heavy and light holes intersect for a certain value of the wave number k. For simplicity, we did not consider in our model the effect of band mixing which eliminates this intersection.

By neglecting the homogeneous and inhomogeneous broadening, the optical gain spectrum caused by the electronic transitions between the given subbands of the conduction band and the valence band in the quantum well is described by the expression [7]

$$g_{cv}(E_{ph}) = \left(\frac{4\pi^2 e^2 \hbar}{ncm_0^2 E_{ph}}\right)|M_{cv}|^2 \rho_{red}(E_{tr})[f_c(E_c) - f_v(E_v)], \quad (1)$$

where E_{ph} is the photon energy; e and m_0 are the free-electron charge and mass respectively; n is the refractive index; c is the speed of light in vacuum; $|M_{cv}|^2$ is the transition matrix element; $\rho_{red}(E_{tr})$ is the reduced density of states

$$\rho_{red}(E_{tr}) = \frac{m_{red}}{2\pi\hbar^2 d}\theta(E_{tr} - E_g); \quad m_{red} = \frac{m_c m_v}{m_c + m_v}; \quad (2)$$

$E_{tr} = E_c - E_v$ is the transition energy (in the absence of broadening; $E_{tr} = E_{ph}$); $E_g = E_{c0} - E_{v0}$ is the forbidden gap; $\theta(E)$ is the theta function [$(\theta(E) \equiv 0$ for $E < 0$, and $\theta(E) \equiv 1$ for $E > 0$]; d is the quantum-well thickness; $f_{c,v}(E) = \{1 + \exp[(E - E_{Fc,\,Fv})/k_B T]\}^{-1}$ is the Fermi–Dirac distribution for electrons in the conduction band and the valence band; E_c and E_v are the energies of states between which the transition takes place,

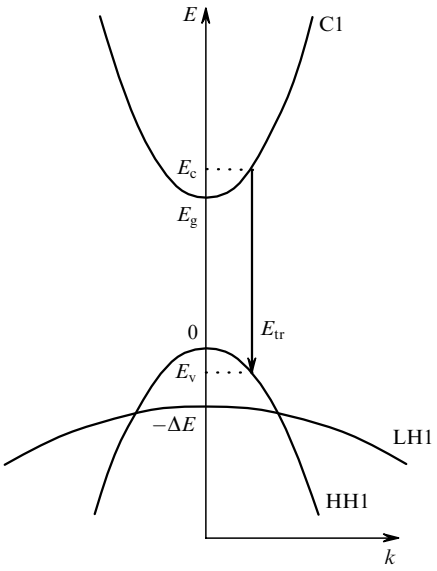

Figure 1. Quantum-well subbands considered in the model: C1: the first conduction subband; LH1 and HH1: the first subbands of the light and heavy hole bands, respectively; E_c, E_v: energy levels between which the transition takes place; E_{tr}: transition energy; E_g: band gap; ΔE: splitting between light and heavy hole bands.

$$E_c = E_{c0} + \frac{\hbar^2 k^2}{2m_c}, \quad E_v = E_{v0} - \frac{\hbar^2 k^2}{2m_v}; \quad (3)$$

E_{c0} and E_{v0} are the energies of the bottom of the conduction and valence band respectively. Hereafter, the electron and hole masses (m_c and m_v) indicate the effective masses corresponding to the motion in the plane of the quantum well.

We assume that the electron wave vector selection rule is observed during the transition. By eliminating k from Eqns (3), we obtain

$$E_c = E_{c0} + \frac{m_{red}}{m_c}(E_{tr} - E_g), \quad E_v = E_{v0} - \frac{m_{red}}{m_v}(E_{tr} - E_g). \quad (4)$$

The interaction of light with an individual electron–hole pair depends on the position of the electric field vector relative to the direction of the electron wave vector. All directions of the wave vector are equivalent in a bulk medium and the total gain is independent of the radiation polarisation. This is not the case for a quantum well [5]. The polarisation dependence of the gain is contained in the transition matrix element which can be written in the form

$$|M_{cv}|^2 = P_{cv}|M_{avg}|^2, \quad (5)$$

where $|M_{avg}|^2$ is the transition matrix element averaged over all polarisations, and P_{cv} is the polarisation factor (having different values for transitions between different subbands).

We will neglect the dependence of these quantities on the transition energy and use their values at the boundaries of the corresponding bands.

Since we are considering two subbands (HH and LH) of the valence band, our expression for the gain must contain two terms of type (1), one for the transition C-HH and the other for the transition C-LH. We will also take into account the homogeneous broadening caused by the intraband relaxation processes by convoluting the expression (1) with the broadened profile $L(\delta E)$. The resulting expression for the gain spectrum has the form

$$g(E_{\rm ph}) = \left(\frac{2\pi e^2 |M_{\rm avg}|^2}{\hbar c d n m_0^2 E_{\rm ph}}\right) \times \sum_{\sigma={\rm lh,hh}} P_{c\sigma} m_{{\rm red}\,\sigma} \int_{E_{g\sigma}}^{\infty} {\rm d}E_{\rm tr} L(E_{\rm ph} - E_{\rm tr}) \left[f_{\rm c}\left(E_{\rm c0} + \frac{m_{{\rm red}\,\sigma}}{m_{\rm c}} \times (E_{\rm tr} - E_{{\rm g}\,\sigma})\right) - f_{\rm v}\left(E_{\sigma 0} - \frac{m_{{\rm red}\,\sigma}}{m_\sigma}(E_{\rm tr} - E_{{\rm g}\,\sigma})\right)\right]. \quad (6)$$

Here, in accordance with Fig. 1, $E_{\rm c0} = E_{\rm g}$, $E_{\rm hh\,0} = 0$, $E_{\rm lh\,0} = -\Delta E$, $E_{\rm g\,hh} \equiv E_{\rm c0} - E_{\rm hh\,0} = E_{\rm g}$, $E_{\rm g\,lh} \equiv E_{\rm c0} - E_{\rm lh\,0} = E_{\rm g} + \Delta E$.

While determining the carrier-induced change in the refractive index, we will take into account two contributions:

$$\Delta n(E_{\rm ph}) = \Delta n_{\rm tr}(E_{\rm ph}) + \Delta n_{\rm fc}(E_{\rm ph}). \quad (7)$$

The first contribution $\Delta n_{\rm tr}$ is associated with the interband transitions C-HH and C-LH, and can be obtained from expression (6) for the gain using the Kramers–Kronig relation

$$\Delta n_{\rm tr}(E_{\rm ph}) = \frac{\hbar c}{2\pi} \int_{-\infty}^{+\infty} \frac{n(E)}{n(E_{\rm ph})} \frac{[g(E) - g(E)|_{N=0}]{\rm d}E}{(E_{\rm ph} - E)E}, \quad (8)$$

where the principal value of the integral is taken. Assuming that $\Delta n \ll n$ and that the gain spectrum width is much smaller than $E_{\rm ph}$, we can write this expression in the form

$$\Delta n_{\rm tr}(E_{\rm ph}) = \frac{\hbar c}{2\pi E_{\rm ph}} \int_0^{+\infty} \frac{[g(E) - g(E)|_{N=0}]{\rm d}E}{(E_{\rm ph} - E)}. \quad (9)$$

Finally, using formula (6) for the gain, we arrive at the following expression for the change in the refractive index:

$$\Delta n(E_{\rm ph}) = \left(\frac{e^2 |M_{\rm avg}|^2}{d n m_0^2 E_{\rm ph}^2}\right) \times \sum_{\sigma={\rm lh,hh}} P_{c\sigma} m_{{\rm red}\,\sigma} \int_{E_{g\sigma}}^{\infty} {\rm d}E_{\rm tr} \tilde{L}(E_{\rm ph} - E_{\rm tr}) \left[f_{\rm c}\left(E_{\rm c0} + \frac{m_{{\rm red}\,\sigma}}{m_{\rm c}} \times (E_{\rm tr} - E_{{\rm g}\,\sigma})\right) - f_{\rm v}\left(E_{\sigma 0} - \frac{m_{{\rm red}\,\sigma}}{m_\sigma}(E_{\rm tr} - E_{{\rm g}\,\sigma})\right) + 1\right], \quad (10)$$

where

$$\tilde{L}(E) \equiv \int_{-\infty}^{+\infty} \frac{L(E'){\rm d}E'}{E - E'}.$$

The second contribution $\Delta n_{\rm fc}$ is the so-called contribution from free carriers. The presence of free charge carriers with an effective mass m^*, charge q, and concentration N introduces the correction to the permittivity of the medium

$$\Delta \varepsilon_{\rm fc}(\omega) = -\frac{4\pi N q^2}{m^* \omega^2}. \quad (11)$$

In our case, there are three types of carriers: the conduction electrons, light holes, and heavy holes. Therefore, assuming once again that $\Delta n \ll n$, we can write

$$\Delta n_{\rm fc}(E_{\rm ph}) = -\frac{2\pi \hbar^2 e^2}{n E_{\rm ph}^2} \left(\frac{N_{\rm c}}{m_{\rm c}} + \frac{N_{\rm lh}}{m_{\rm lh}} + \frac{N_{\rm hh}}{m_{\rm hh}}\right). \quad (12)$$

The Fermi quasilevels $E_{\rm Fc,\,Fv}$ in the conduction and valence bands are related to the concentrations of electrons and holes in the quantum well. Assuming the overall electroneutrality of the quantum well (i.e., the equality of the above-mentioned concentrations), this relation for parabolic bands can be written in the form

$$N = \frac{m_{\rm c} k_{\rm B} T}{\pi \hbar^2 d} \ln\left[1 + \exp\left(\frac{E_{\rm Fc} - E_{\rm c0}}{k_{\rm B} T}\right)\right], \quad N = \sum_{\sigma={\rm lh,hh}} \frac{m_\sigma k_{\rm B} T}{\pi \hbar^2 d} \ln\left[1 + \exp\left(-\frac{E_{\rm Fv} - E_{\sigma 0}}{k_{\rm B} T}\right)\right]. \quad (13)$$

Eqns (6) and (13) allow us to determine the gain spectrum for a given carrier concentration in the quantum well. Unfortunately, the carrier concentration N cannot be measured directly in the experiment. Hence a comparison of the results of calculations with the experimental data requires a relation between N and the pump current density J. While deriving this relation, we shall consider only the radiative recombination mechanism for the carriers, i.e., a recombination through spontaneous emission. Modifying the formula presented in [7] for the case of our three-band model, we finally arrive at the expression

$$J = \left(\frac{2e^3 n |M_{\rm avg}|^2}{\pi \hbar^4 c^3 m_0^2}\right) \times \sum_{\sigma={\rm lh,hh}} m_{{\rm red}\,\sigma} \int_{E_{g\sigma}}^{\infty} {\rm d}E_{\rm tr} E_{\rm tr} f_{\rm c}\left(E_{\rm c0} + \frac{m_{{\rm red}\,\sigma}}{m_{\rm c}}(E_{\rm tr} - E_{{\rm g}\,\sigma})\right) \times \left[1 - f_{\rm v}\left(E_{\sigma 0} - \frac{m_{{\rm red}\,\sigma}}{m_\sigma}(E_{\rm tr} - E_{{\rm g}\,\sigma})\right)\right]. \quad (14)$$

3. Comparison of theoretical and experimental results and discussion

To determine the numerical parameters used in expressions (1)–(14), we measured the material gain and the correction to the refractive index of the active layer. Laser diodes with a broad active region were used in these measurements. The samples were prepared at the Ferdinand Braun Institut für Höchstfrequenztechnik (FBH), Berlin, on the basis of a heterostructure whose parameters are given in Table 1. The laser cavity was 2 mm long and the transverse size W of the pumped region (along the p–n junction) was 100 μm. The latter circumstance is essential for such experiments since it is only for such samples that the optical beam can be

assumed to propagate entirely in a homogeneous medium. The majority of earlier similar measurements were made on samples with a narrow ($W \leqslant 4$ μm) active zone, in which the transverse profile of the optical wave covers regions with different concentrations of injected carriers. In such samples, a contribution to the resultant mode gain comes from spatial regions with different values of the material gain and different spectral dependences. Thus, the experimentally measured mode gain is a 'convolution' over different spectral curves corresponding to different spatial regions. It is quite difficult to single out the material gain corresponding to a single value of the carrier concentration from such data.

Table 1. Characteristics of the heterostructure layers for the investigated laser.

Layer	Material	Thickness/nm	Doping/cm^{-3}
Contact	p–GaAs^{+}	150	2×10^{19}
Emitter	P–$Al_{0.25}Ga_{0.75}As$	1400	10^{18}
Waveguide	p–GaAs	400	10^{17}
Intermediate	$GaAs_{0.85}P_{0.15}$	14	undoped
Active region	InGaAs	8	undoped
Intermediate	$GaAs_{0.85}P_{0.15}$	14	undoped
Waveguide	n–GaAs	350	10^{17}
Emitter	N–$Al_{0.25}Ga_{0.75}As$	1500	10^{18}
Buffer	n–GaAs	300	2×10^{18}
Substrate	n–GaAs	–	–

It was noted above that it has become possible to use samples with a wide active zone for these purposes due to a high technological level that has been attained by now. In particular, a high degree of spatial homogeneity (along the p–n junction) could be achieved for the heterostructure used for preparing the samples.

The field distribution in the vertical direction (at a right angle to the p–n junction) is strictly constant. Therefore, the passage from the mode gain being measured to the material gain is made by simple recalculation using the optical confinement factor, which is a constant for the given structure. Its value is calculated from the solution of the waveguide problem and its accuracy is verified from the coincidence of the calculated and measured far-field laser radiation intensity distributions. For the structure studied here, the optical confinement factor was found to be 0.0132. The mode gain was measured using the modified Hucky–Paoli technique described in [10, 11].

Figures 2 and 3 show the results of comparison of theoretical and experimental data. Table 2 contains the complete set of parameters used in calculations, as well as their values for which the best fit of the theoretical and experimental results was achieved. The effective masses m_c, m_{hh} and m_{lh} in the plane of the quantum well were calculated using the data on Luttinger parameters and formulas presented in Ref. [6]. The polarisation factors P_{c-hh} and P_{c-lh} correspond to TE polarisation of radiation. The value for the transition matrix element is close to that given in [5]. The band gap E_g, the splitting ΔE of the subbands of light and heavy holes and the width of the

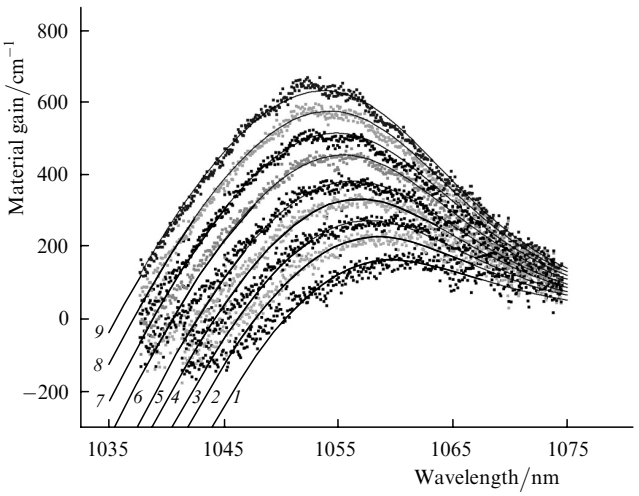

Figure 2. Comparison of experimental and theoretical gain spectra; experimental data (dots) correspond to the pump current density from 80 to 120 A cm^{-2} with a step of 5 A cm^{-2} (in the upward direction); for calculated dependences (curves) $N = 1.11 \times 10^{18}$ [curve (*1*)], 1.14×10^{18} (curve (*2*)], 1.16×10^{18} [curve (*3*)], 1.186×10^{18} [curve (*4*)], 1.207×10^{18} [curve (*5*)], 1.237×10^{18} [curve (*6*)], 1.262×10^{18} [curve (*7*)], 1.287×10^{18} [curve (*8*)], and 1.31×10^{18} cm^{-3} [curve (*9*)].

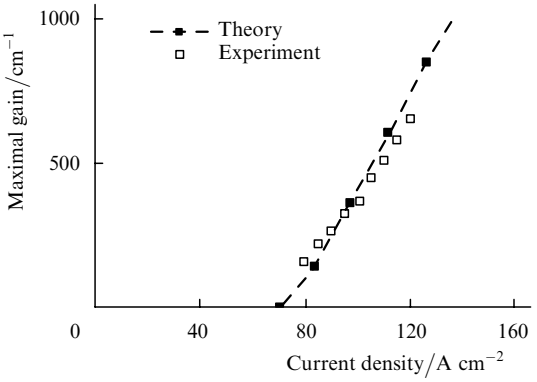

Figure 3. Theoretical and experimental dependences of the gain maximum on the pump current density.

homogeneous profile were determined from a comparison of the theoretical and experimental curves. The homogeneous profile $L(\delta E)$ has the form of a hyperbolic secant with the FWHM $\Delta E_{1/2}$.

Note that a good coincidence of theoretical and experimental dependences for the material gain is observed in the shape of the spectral curves (Fig. 2), while the agreement is satisfactory for the differential gain (Fig. 3). The discrepancy between the theoretical values of the differential gain and the experimental data is about 30 %, which is quite acceptable for this kind of calculations and measurements. Our earlier attempts to calculate the gain in an even simpler two-band model did not lead to results like those obtained using the three-band model. Variation of the numerical values of parameters in the two-band model did not provide a good coincidence of theory with the experiment. In this connection, it can be stated that the three-band model is

Table 2. Values of parameters used in calculations.

Parameter	E_g/eV	ΔE/meV	m_c	m_{hh}	m_{lh}	$2\lvert M_{avg}\rvert^2 m_0^{-1}$/eV	P_{c-hh}	P_{c-lh}	$\Delta E_{1/2}$/meV	n	T/K	d/nm
Value	1.169	20	0.06 m_0	0.08 m_0	0.17 m_0	16.7	1.5	0.5	25	3.45	300	8

apparently the simplest model that makes it possible to obtain theoretical values for the complex permittivity of the active layer that are suitable for numerical simulation of parameters of the new injection lasers being developed.

The data shown in Fig. 2 demonstrate the blue shift of the gain band with increasing the pump current. This is a typical behaviour of the active semiconducting medium associated with successive filling of the lower energy states by carriers (usually electrons) with increasing the pump current. The narrowing of the band gap due to Coulomb interaction between carriers is often taken into account in an analysis of the spectral profile of the gain. This effect leads to the red shift of the gain band with increasing the carrier concentration, which is opposite to the blue shift caused by the filling of the lower energy states by carriers. *Ab initio* calculation of correction to the total particle energy associated with Coulomb interaction between particles under conditions characteristic of the active medium is extremely difficult. Indeed, the accuracy of the calculations must be quite high since a small correction is being determined. On the other hand, a high degree of precision is possible only if the analysis is carried out using the many-particle theory which has been used for solving only a few problems. This is probably the reason behind the considerable discrepancy in the results of calculations made by different authors. This was noted in [9] where various dependences of correction on the charge carrier concentration N ($\sim N$, $\sim N^{1/2}$, $\sim N^{1/3}$) were described.

The results obtained in this work (see Fig. 2) indicate that the effect of the Coulomb interaction is quite weak. In the pump range considered by us, it does not affect qualitatively the behaviour of the gain spectrum. The mean value of the decrease in the band gap can be taken into account by appropriately changing the model parameter E_g (see Table 2).

An intermediate result of calculations is the dependence of the current density J on the electron concentration N defined by Eqns (13), (14). Figure 4 shows the results of such calculations. One can see that, for concentrations N lower than 10^{18} cm^{-3}, the bimolecular recombination approximation in which the current density J is a quadratic function of N is applicable. This classical result is due to a low degeneracy of charge carriers. For higher concentrations, the degeneracy of carriers is significant and the dependence $J(N)$ becomes virtually linear for values of N exceeding 2×10^{18} cm^{-3}. From this dependence, the average lifetime $\tau_{avg}(N) = edN/J$ and the differential lifetime $\tau_{diff}(N) = ed(dN/dJ)$ of charge carriers can be obtained; the corresponding curves are shown in Fig. 5.

In this work we assume the quantum well to be electrically neutral. The presence of a nonzero charge in the quantum well due to different doping levels of p- and n-emitter layers of the heterostructure (such a possibility was noted in [12]), i.e., the excess of one type of carriers, will lead to a decrease in the nonlinearity region in the $J(N)$ dependence (Fig. 4) due to an increase in degeneracy. In this case, the relation between J and N may be linear and not quadratic even for small pump current densities.

It should also be noted that the energy difference between the first and second subbands of the heavy hole band in the quantum well under investigation is of the same order of magnitude as the quantity ΔE; consequently, strictly speaking, we must also consider the second subband (HH2) of the heavy hole band along with subbands HH1

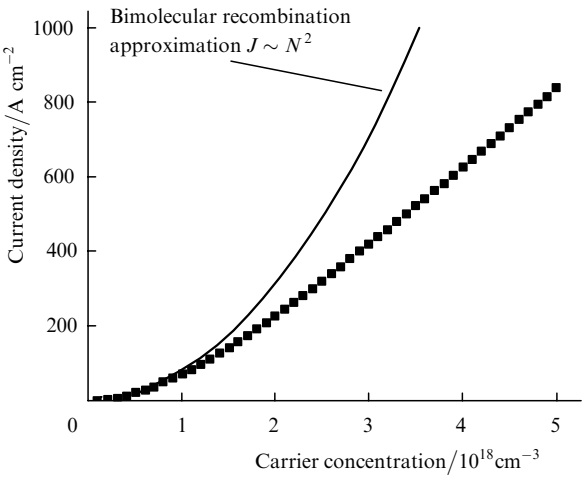

Figure 4. Theoretical dependence of the density of radiative recombination current on the carrier concentration.

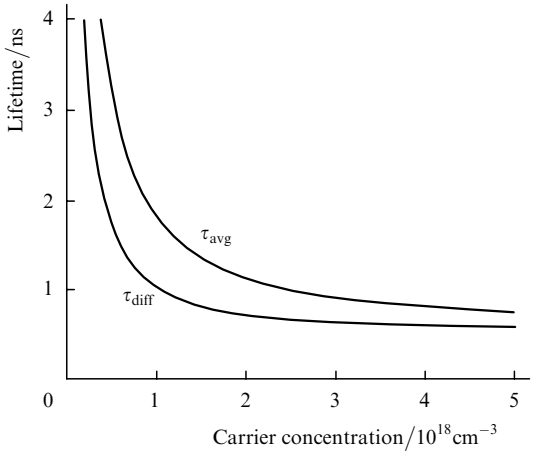

Figure 5. Theoretical dependences of the average and differential lifetime of carriers on their concentration.

and LH1. However, since optical transitions C1 – HH2 are forbidden (the overlap integral for the envelope functions is zero), the subband HH2 makes zero contribution to the gain and to the spontaneous recombination intensity; it acts as a passive reservoir for holes. The inclusion of this subband in the model virtually does not affect the resultant gain spectra and the $g(J)$ dependence, but leads to an increase in the carrier lifetime by approximately 20 %. One more circumstance, which is ignored in this work and which may affect the form of the $J(N)$ dependence, is worth noting. We are speaking of the transitions induced by enhanced spontaneous emission (superluminescence). However, these transitions are significant only in the vicinity of the lasing threshold as a rule.

The values of parameters determined by us also make it possible to calculate the change in the refractive index of the active layer in the case of injection of carriers in accordance with relations (7) – (12). To simplify a comparison with experiment, it is more convenient to consider the quantity $\partial n/\partial J$. The calculated spectral dependences of $\partial n/\partial J$ are presented in Fig. 6.

The comparison shows that the experimental value of $\partial n/\partial J$ at the lasing wavelength exceeds the calculated value

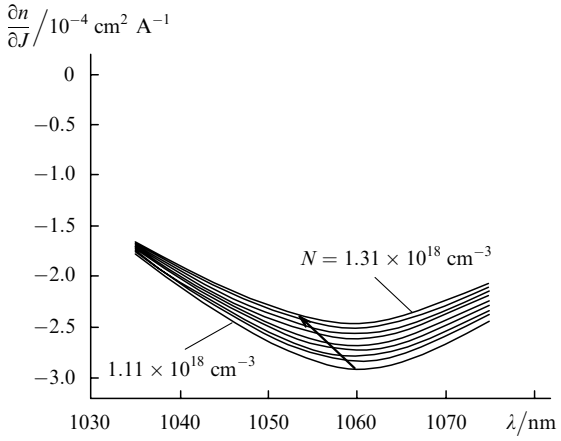

Figure 6. Theoretical variation of the refractive index, induced by carriers. The arrow shows the shift of the gain maximum as a result of the corresponding increase in the carrier concentration; the values of N are the same as in Fig. 2.

approximately by a factor of 1.5. Most likely, this discrepancy is due to a difference between the calculated gain spectrum and the actual spectrum in the spectral region outside the simulation range.

The possibility of simultaneous calculation of quantities $\partial n/\partial J$ and $\partial g/\partial J$ also allows us to determine the α factor of the amplitude–phase coupling (Henry factor) from the relation

$$\alpha = -\frac{4\pi}{\lambda}\frac{(\partial n/\partial J)}{(\partial g/\partial J)}. \qquad (15)$$

Figure 7 shows the spectral dependence of α obtained in this way. This dependence exhibits the expected behaviour, i.e., an increase in the value of the α factor observed by many authors (see, for example, [13, 14]) upon an increase in the wavelength. Note that the accuracy of calculation of α is apparently determined by the accuracy of calculation of $\partial n/\partial J$. Consequently, the real values may exceed those presented in Fig. 7 by 50 %.

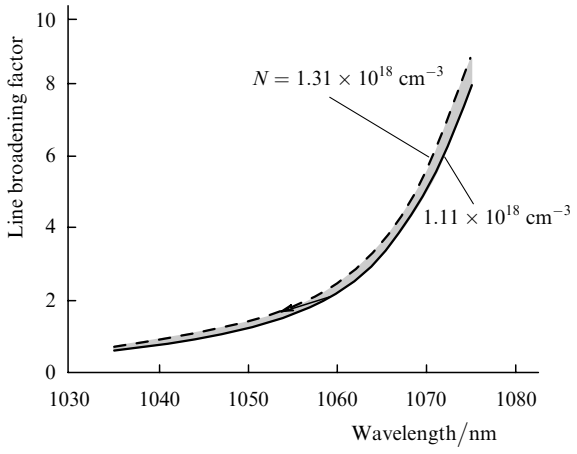

Figure 7. Theoretical line broadening factor. The arrow shows the shift of the spectral gain peak as a result of the corresponding increase in the carrier concentration.

4. Conclusions

The results obtained in this paper indicate that the proposed three-band model is apparently the simplest model that can be used for calculating corrections to the complex permittivity of the InGaAs-based active layer upon injection of excess charge carriers into it. Of course, preliminary measurements, which can be made for any heterostructure, are required for obtaining the parameters characterising the active layer. Having obtained a set of parameters in this way, we can carry out numerical simulation of injection lasers of various types. The only condition for the applicability of such an approach is the use of the active layer of the same composition for which the numerical values of the parameters were obtained. Such a calculation procedure may appear as ineffective at first glance since it must be based on experiment in one way or another. However, it should be noted that a change in the laser design and in the very heterostructure that may contain different numbers of passive layers of various composition and thickness may lead to a more than an order of magnitude change in the laser parameters for the same active region. It is such parameters of the laser (e.g., the threshold current, light–current characteristics and the near- and far-field radiation intensity distributions) that can be simulated to a high degree of accuracy using the approach described above.

Obviously, this approach (which is based on the use of the three-band model and a limited number of numerical parameters) can be also extended to active III–V semiconductors with a different composition. This makes it possible to optimise the parameters of the injection lasers being developed with a minimum expenditure on laborious and expensive technological experiments involving the preparation of heterostructures and lasers based on them.

Acknowledgements. This research was partially supported by FBH under an agreement between the P.N. Lebedev Physics Institute of Russian Academy of Sciences and FBH, as well as by the Presidium of the Russian Academy of Sciences under the programmes 'Low-dimensional Quantum Structures' and 'Semiconductor Lasers'. The authors thank the staff of FBH for providing laser samples and for useful discussions.

References

1. *Properties of Lattice-Matched and Strained Indium Gallium Arsenide, EMIS Datareviews Ser. No. 8* (London: INSPEC, 1990).
2. *Properties of Aluminum Gallium Arsenide, EMIS Datareviews Ser. No. 7* (London: INSPEC, 1990).
3. Adachi S.J. *Appl. Phys.*, **58**, R1 (1985).
4. Afromowitz M.A. *Solid State Commun.*, **15**, 59 (1974).
5. Corzine S.W., Yan R.-H., Coldren L.A., in *Quantum Well Lasers*. Ed. by P.S. Zory (San Diego: Acad. Press Inc., 1993).
6. Chow W.W., Koch S.W., Sargent M. *Semiconductor-Laser Physics* (New York: Springer-Verlag, 1994).
7. Yan R.H., Corzine S.W., Coldren L.A., Suemune I. *IEEE J. Quantum Electron.*, **26**, 213 (1990).
8. Ma T.A., Li Z.-M., Makino T., Wartak M.S. *IEEE J. Quantum Electron.*, **31**, 29 (1995).
9. Balle S. *Phys. Rev. A*, **57**, 1304 (1998).
10. Bogatov A.P., Boltaseva A.E., Drakin A.E., Belkin M.A., Konyaev V.P. *Kvantovaya Elektron.*, **30**, 315 (2000) [*Quantum Electron.*, **30**, 315 (2000)].

11. Bogatov A.P., Boltaseva A.E., Drakin A.E., Belkin M.A., Konyaev V.P. *Fiz. Tekh. Poluprov.*, **34**, 1258 (2000).
12. Chelnyi A.A. *Private communication* (2003).
13. Schönfelder A., Weisser S., Ralston J.D., Rosenzweig J. *IEEE Photon. Techn. Lett.*, **6**, 891 (1994).
14. Lui G., Jin X., Chuang S.L. *IEEE Photon. Techn. Lett.*, **13**, 430 (2001).